Adsorption Behavior of As(III) onto Chitosan Resin with As(III) as Template Ions

Bingjie Liu, Xin Lv, Dongfeng Wang, Ying Xu, Li Zhang, Yujin Li

College of Food Science and Engineering, Ocean University of China, Qingdao 266003, China

Received 12 May 2011; accepted 21 August 2011
DOI 10.1002/app.35528
Published online 17 December 2011 in Wiley Online Library (wileyonlinelibrary.com).

ABSTRACT: A novel, biobased chitosan resin was successfully synthesized, characterized, and applied for the selective removal of As(III) from aqueous solutions. Batch adsorption experiments were performed to evaluate its adsorption conditions, selectivity, and reusability. The results showed that the maximum adsorption capacity was 2.16 mg/g, observed at pH 6 and 40°C. Equilibrium adsorption was achieved within 8 h. The kinetic data, obtained at optimal pH 6, could be fitted with a pseudosecond order equation. Adsorption process could be well described by Langmuir adsorption isotherm model and the maximum adsorption capacity calculated from Langmuir equation was 4.45 mg/g. The selectivity coefficient of As(III) ions and other metal cation onto As-ICR indicated an overall preference for As(III) ions, which was much higher than nonimprinted chitosan resins. Finally, the adsorption mechanisms were studied by Fourier transform infrared spectra, X-ray diffraction, and differential scanning calorimetry analysis. The result reveals that the adsorption of As-ICR for As(III) is a chelation process. These results earlier confirmed that As-ICR is a very promising sorbent for selective adsorption of As(III) ions from aqueous solutions. © 2011 Wiley Periodicals, Inc. J Appl Polym Sci 125: 246–253, 2012

Key words: As(III); ion imprinted; chitosan resin; adsorption; heavy metals

INTRODUCTION

Arsenic is a geogenic water menace affecting millions of people all over the world and is regarded as the largest mass poisoning in history. Permanent arsenic intake leads to chronic intoxication, and prolonged arsenic exposure can damage the central nervous system, liver, skin and results in the appearance of diverse types of cancer, such as hyperkeratosis, lung, and skin cancer.[1,2] People drinking water or eating food, contaminated with arsenic concentrations equal to or greater than 50 μg/L are prone to increase the risks of lung and bladder cancer and of arsenic-associated skin lesions.[3] World Health Organization and the U.S. Environmental Protection Agency have revised the maximum contaminant level of arsenic in drinking water from 50 to 10 μg/L.[4] Therefore, removal and recovery of arsenic from contaminated water has attracted more and more attention for environmentalists.

Several treatments have been developed for the removal of arsenic from contaminated water.[5,6] The common methods adopted for the treatment of arsenic-contaminated water contain flotation,[7,8] precipitation with sulfide,[9] coagulation,[10] oxidation of As(III) followed by removal of total arsenic using ferric hydroxide,[11] filtration, and ion exchange.[12] However, ion exchange plants have high maintenance and operation costs. Chemical precipitation is capable of removing trace levels of heavy metal ions but its precipitates are difficult to be separated due to their settling characteristics.[13] Adsorption has been proved to be a highly efficient and relatively low-cost technique for the treatment of heavy metal contaminated waters. Hence, a nontoxic, biodegradable, renewable adsorption material is urged to be found or synthesized to adsorb heavy metal from contaminated waters.

Chitosan (CTS) is the *N*-deacetylation product of chitin, a biopolymer that can be formulated into resins and films, the major component of the shells of crustacean organisms and the second most abundant naturally occurring biopolymer next to cellulose. CTS has biological and chemical properties, such as nontoxicity, biocompatibility, high chemical reactivity, chelation, and adsorption properties.[14–16] The presence of amine groups make CTS unique among biopolymers, for example, its cationic behavior in acidic solutions and its affinity for heavy metal

Correspondence to: D. Wang (wangdf@ouc.edu.cn).

Contract grant sponsor: Ocean Public Welfare Scientific Research Special Appropriation Project; contract grant number: 201005020.

Contract grant sponsor: National Natural Science Foundation of China; contract grant numbers: 20807040, 30972289.

Contract grant sponsor: International cooperation project; contract grant number: 2010DFA31330.

© 2011 Wiley Periodicals, Inc.

ions.[17,18] Nowadays, CTS is an excellent adsorbent and widely used in the form of resin to adsorb heavy metal ions from contaminated water.[19–21] However, the selectivity of CTS resin for specified metal ions was very low, it might adsorb a number of essential mineral elements besides heavy metal ions simultaneously, which restricted its application in the removal of specific heavy metal ions from liquid food, such as beverage, hydrolysate and so on.

Molecular imprinting is an emerging technology that has gained much attention in generating recognition sites by reversible immobilization of template molecules on crosslinked macromolecular polymer matrices. Due to the interaction between monomers and templates, the imprinted materials possess predetermined arrangement of ligands and tailored binding pockets, which behave affinity and selectivity for the template molecule over other structurally related compounds.[22–24] So far, many metal ions imprinted polymers have been prepared, including Dy(III),[25] Gd(III),[26] UO_2(II),[27] Pd(II),[28] Cu(II),[29] Zn(II),[30,31] Al(III),[32] Ni(II),[33] Ca(II),[34] and Mg(II)[35] imprinted ones.

The aim of this study was to prepare As(III)-imprinted CTS resin to evaluate the adsorption property. The adsorption mechanisms of As-ICR for As(III) have also been characterized by means of Fourier transform infrared spectra (FTIR), X-ray diffraction (XRD), and differential scanning calorimetry (DSC) spectra.

MATERIALS AND METHODS

Materials

CTS (CTS, degree of deacetylation 92.2%, MW5.0 $\times$ 10^5 Da) was purchased from Shandong Hecreat Marine Bio-tech (Qingdao, China). Metal ion standard solutions were all obtained from National Steel Material Test Center (Beijing, China). Acetic acid, liquid paraffin, ethyl acetate, glutaraldehyde, sodium borohydride, hydrochloric acid, and all the other reagents used in this experiment were of analytical grade or better and used as received without further purification. Deionized distilled water (Milli-Q, Millipore) was used throughout the experiments.

Preparation of As(III)-imprinted CTS resin

The experimental procedure for the preparation of As(III)-imprinted CTS resin was described in detail as follows:

First, a total of 10.0 g CTS was added to 200 mL 100 mg/L As(III) aqueous solution, shaking for 24 h at 40°C. The mixture was filtered under reduced pressure, and then the residue was washed with deionized distilled water until As(III) could not be detected in the filtrate. The residue was dried in a vacuum oven at 50°C.

Thereafter, the earlier product was swelled in 200 mL 2% acetic acid aqueous solution. As for the preparation of a dispersion phase, liquid paraffin and ethyl acetate was heated up to 50°C, stirring for 20 min at 300 rpm. After that, the system was heated up to 60°C, stirring for 3 h at 175 rpm, meanwhile, glutaraldehyde was added as a crosslinking agent to generate polymeric resins. The prepared resins were thoroughly washed with petroleum ether, acetone, ethanol, and deionized distilled water in sequence to remove any unreacted fraction.[36] And then, the template molecule As(III) was removed from the resins using 0.5 mol/L HCl. The wet resins were collected and dried at 50°C, abbreviated as As-ICR.

As a control, nonimprinted CTS resin (NICR) was prepared under identical experimental conditions without adding As(III).

Characterization

FTIR (Nexus 470, Nicolet) of As-ICR before and after As(III) adsorption were obtained and all samples were prepared as a potassium bromide tablet (1 mg of the powder was blended with 100 mg of IR-grade KBr in an agate mortar and pressed into a tablet).

XRD (D8 ADVANCE, Bruker AXS) analysis of the powdered samples were performed using an X-ray powder diffractometer with Cu anode, running at 40 kV and 30 mA, scanning from 5° to 50° at 2°/min.

The DSC (200PC, Netzsch) of the samples was carried out using a calorimetry (temperature range 25°C–400°C). The heating rate was 10°C/min and the cooling nitrogen gas was 20 mL/min.

Adsorption experiments

Batch adsorption experiments were carried out in 50 mL Erlenmeyer flasks. The amount of adsorbent used was 0.1 g and volume of 50 mg/L As(III) aqueous solution was maintained at 25.0 mL. The pH of the solution was adjusted by adding 1.0 mol/L NaOH or 1.0 mol/L HCl. The pH value was measured using a Delta 320 pH meter. The batch experiments were carried out at a constant temperature and the equilibration time was 24 h. After the adsorption equilibration, the adsorbent was separated through filtration. As(III) concentration of the filtrate was measured with a flame atomic absorption spectrophotometer (AA-6800, Shimadzu Ins), equipped with a hydride vapor generator (HVG-1, Shimadzu Ins) at 193.7 nm wavelengths, using 1.8 wt % $NaBH_4$ and 5 mol/L HCl solution as reducing reagents, the concentration of other metal ions was measured with flame atomic absorption spectrophotometer.

The amount of As(III) ions adsorbed per unit mass of As-ICR was calculated by using the following equation:

$$q_e = \left(\frac{C_i - C_e}{W}\right)V \quad (1)$$

where, q_e is the adsorption capacity of the resins (mg/g); C_i and C_e are the concentrations of As(III) in the initial and equilibrium solution (mg/L), respectively; V is the volume of the aqueous solution (L) and W is the mass of dry resins (g).

Selective adsorption studies

The selectivity of As-ICR for As(III) ions over other metal ions were evaluated from the selectivity coefficient ($\beta_{As^{3+}/M^{n+}}$), which was determined by incubating 0.1 g of resins with 25 mL 50 mg/L mixed heavy metal ions under identical conditions. The selectivity coefficient is defined as[37]:

$$\beta_{As^{3+}/M^{n+}} = \frac{D_{As^{3+}}}{D_{M^{n+}}} \quad (2)$$

where, $D_{As}{}^{3+}$ and $D_M{}^{n+}$ are the distribution ratios of the As(III) ions and other coexistent metal ions, respectively. The distribution ratio (D) was calculated by using the following equation:

$$D = \frac{C_i - C_e}{C_e} \times \frac{V}{W} \quad (3)$$

where, C_i and C_e are the concentrations of metal ions in the initial solution and equilibrium solution (mg/L), respectively; V is the volume of the aqueous solution (L) and W is the mass of dry resins (g).

Desorption and regeneration studies

The regeneration study is very important since the economic success of the adsorption process depends on the regeneration of adsorbent. In the present study, several solvents/solutions were tried to regenerate As-ICR. Out of the solvents/solutions, 0.5 mol/L HCl aqueous solution was found to be effective in desorbing As(III) ions from the loaded As-ICR. The As-ICR was regenerated using 0.5 mol/L HCl aqueous solution, the procedure was repeated for many times until As(III) could not be detected in the filtrate. Then, As-ICR was washed thoroughly with deionized distilled water to a neutral pH. The regenerated As-ICR was reused in the following adsorption experiments and the procedure was repeated for five times by using the same As-ICR.

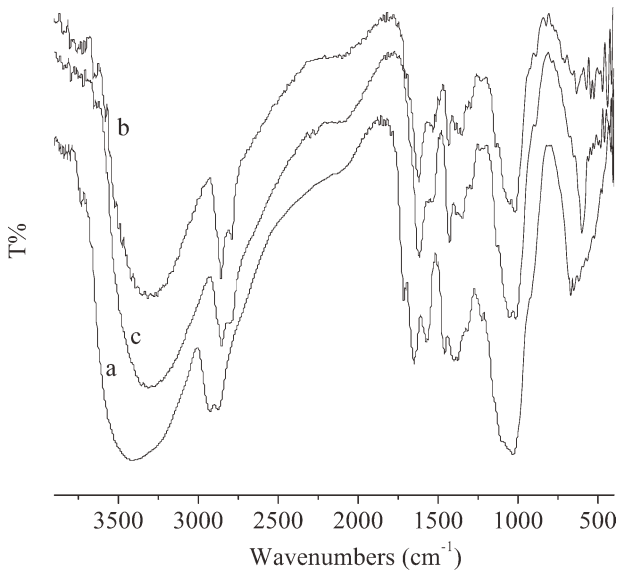

Figure 1 FTIR spectra of (a) NICR; As–ICR before (b); and after (c) As(III) adsorption.

RESULTS AND DISCUSSION

Characterization

FTIR analysis

The FTIR spectra of NICR (a); As-ICR before (b) and after (c) arsenic adsorption are shown in Figure 1. The wide absorb band at 3330 cm^{-1}, corresponding to the stretching vibration of —NH_2 groups and —OH groups, shows a significant shift to higher wave numbers. The bands at 2922 and 2857 cm^{-1}, corresponding to the stretching vibration of —CH_3 and —CH_2 groups, strengthen [Fig. 1(b)]. In contrast, after the crosslinked template resin formed, these peaks weakened and shifted to higher wavenumbers evidently [Fig. 1(c)], according to Fig. 1(a) and Fig. 1(b), the absorb bands at 1028 cm^{-1}, associated with the stretching of C—N bond, weakened and shifted to higher wave numbers, which indicated the formation of N—As coordination bonds in the crosslinked reaction.

The absorb bands at 1077 cm^{-1}, associated with the stretching of the secondary hydroxyl groups, have a significantly downward shift [Fig. 1(b,c)] and the intensity become stronger. The absorb bands at 1152 cm^{-1}, corresponding to the stretching of C—N bond weaken and shifted to higher wave numbers, which indicated the formation of N—As coordination bond in the adsorption process. These results revealed that the amino and hydroxide groups in As-ICR participated in the coordination with arsenic.

The absorb bands observed at 502 and 449 cm^{-1}, assigned to stretching vibration of N—As and O—As, reconfirmed that the amino groups and the hydroxyl groups participated in the coordination process.

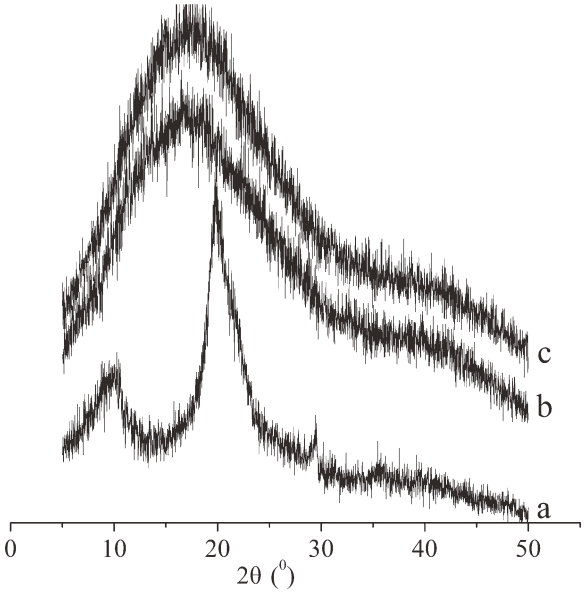

Figure 2 XRD powder patterns of (a) CTS, (b) NICR, and (c) As–ICR.

From the earlier FTIR spectra analysis, it can be concluded that the amino groups (—NH_2) and the hydroxyl groups (C_6—OH) on CTS chains serve as the coordination sites.

XRD analysis

XRD is an effective method for the investigation of resins. Figure 2 shows that the XRD patterns of CTS (a), NICR (b), and As-ICR (c), respectively. The XRD pattern of CTS shows two typical crystalline diffraction peaks at 11.6° and 20.3°, respectively, however, the crystalline peak at 11.6° was disappeared after crosslinked into CTS resins because of amine groups were formed into Schiff base to destroy the amine groups and hydrogen bonds; the diffraction peaks at 20.3° waken and become wider after the crystalline structure was destroyed. According to the results of XRD and FTIR, it can be concluded that the crystalline structure of CTS was destroyed after formed into resins and new structures were formed among amine, hydroxyl groups, and As(III).

DSC analysis

Figure 3 depicts the DSC curves for purified CTS (a), NICR (b) and As-ICR (c). In the curve of Figure 3, an endothermic peak at 70°C can be ascribed to the loss of water. The second thermal event may be related to the decomposition of amine (GlcN) units with correspondent exothermic peak at 295°C.[38]

CTS has two kinds of hydrogen bonds; one is between the tertiary carbon hydroxyl groups and the quintus carbon—oxygen atom, and the other is between the sextuplicate carbon hydroxyl groups

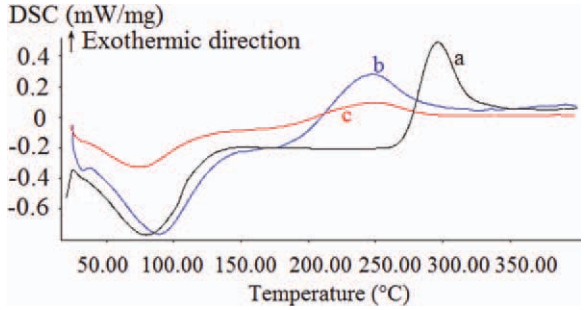

Figure 3 DSC spectra of (a) CTS, (b) NICR, and (c) As–ICR. [Color figure can be viewed in the online issue, which is available at wileyonlinelibrary.com.]

and amino groups.[39] Therefore, CTS has both good crystallinity and good thermal stability. When the crosslinking CTS resins are prepared, the amino groups will react with glutaraldehyde to form Schiff base, destroying the hydrogen bond of CTS [Fig. 3(b,c)]. Consequently, the crystallinity and thermal stability of CTS will decrease. In other word, As-ICR and NICR are less stable than CTS powder under heating condition.

Effect of pH on adsorption

The pH of the aqueous solution, the most important parameter on adsorption studies, strongly affects the adsorption property of resins for heavy metal ions. Metal ions are pH-dependently adsorbed onto non-specific and specific sorbents.[40] The adsorption process of metal ions was sensitive to pH and usually did not occur at low pH.[41] Hence, the effect of pH on chelation between As-ICR and As(III) was investigated.

As seen from Figure 4, the adsorption capacities of both resins for As(III) ions were increased

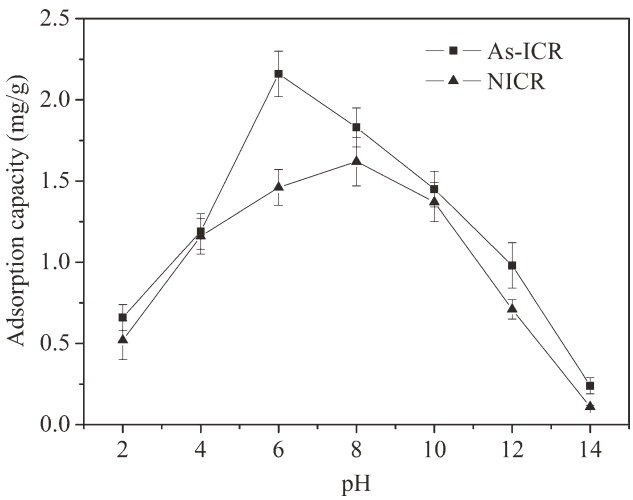

Figure 4 Relationship between adsorption capacities and pH (conditions: initial As(III) concentration 50 mg/L, adsorbent addition 0.1 g, shaking for 24 h at 40 °C).

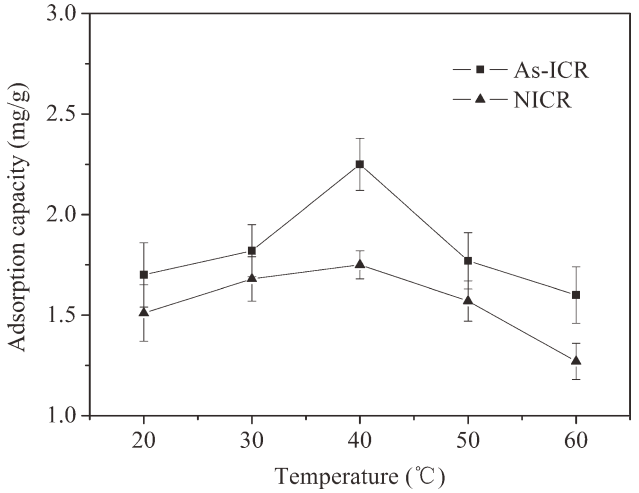

Figure 5 Relationship between adsorption capacity and Temperature (conditions: initial As(III) concentration 50 mg/L, adsorbent addition 0.1 g, shaking for 24 h at pH 6).

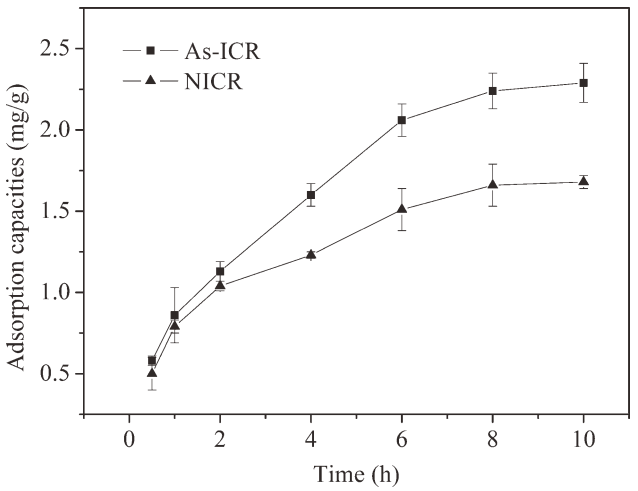

Figure 6 Relationship between adsorption capacity and contact time (conditions: initial As(III) concentration 50 mg/L, adsorbent addition 0.1 g, at pH 6, 40°C).

significantly with the increase of pH below 6, but then leveled off at around pH 6.0–14.0. The maximum adsorption values for As(III) ions onto As-ICR and NICR were 2.16 mg/g and 1.62 mg/g, respectively, from which the imprinting effect is greatly observed. At the low pH (pH < 6), amine groups of CTS were ionized, the decrease of the adsorption capacities can be attributed to the competitive binding of H^+ and As(III) ions to the amine groups.[42] The adsorption capacity increased with the pH increasing, at the high pH, As(III) existed in the form of $H_2AsO_3^-$,[43] the increase of the adsorption capacity can be owed to electrostatic attraction. Hence, pH 6 was chosen as the optimal pH in the following experiments.

Effect of temperature on adsorption

The adsorption capacity of As-ICR for As(III) increased as the temperature is raised from 20 to 40°C (Fig. 5), which was similar to NICR. It's apparent that at the lower temperature (<40°C), the adsorption of As(III) onto As-ICR or the formation of As-ICR with As(III) complexes is favored. However, when the temperature exceeded 40°C, a high temperature favored desorption or dechelation, which indicating that 40°C was the optimal temperature for the adsorption of As(III) onto As-ICR. The results indicated that the adsorption was an endothermic process; hence, 40°C was chosen as the optimal temperature in the following experiments.

Kinetics of As(III) ions adsorption

To achieve the proper design of an adsorbent, the adsorption equilibrium needs to be supplemented with adsorption kinetics, which offers information on the rate of metal adsorption.[44] The time required to achieve adsorption equilibrium for As(III) ions from aqueous solutions was determined. The relationship between adsorption capacity and contact time was described in Figure 6. As can be seen from Figure 6, the initial adsorption rate of the resin was very fast, due to the smaller mass transfer resistance on the surface with the continuation of adsorption. After this initial adsorption period, the adsorption equilibrium was gradually achieved within 8 h. The faster adsorption rate compared with other adsorbents reported elsewhere could be attributed to the absence of internal diffusion resistance.[45]

The adsorption kinetics of As(III) ions onto the resins were analyzed on the basis of the pseudosecond order kinetic model, which is expressed as:

$$\frac{t}{q_t} = \frac{1}{K_2 q_e^2} + \frac{t}{q_e} \tag{4}$$

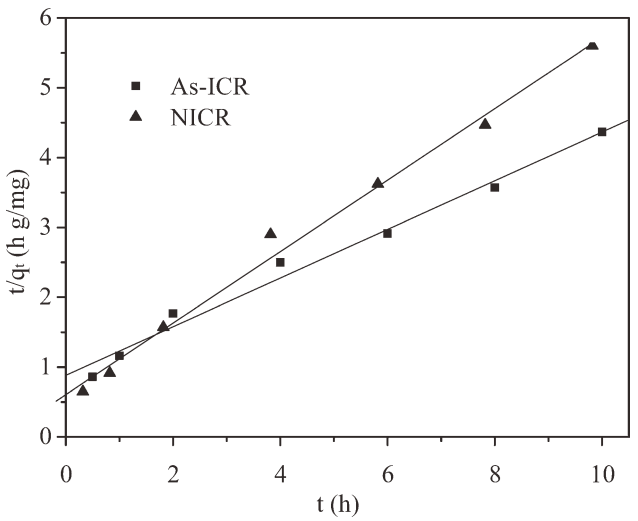

Figure 7 Plots for pseudosecond order kinetic modeling.

TABLE I
Pseudosecond Kinetic Model Rate Constants for the Adsorption of As(III) onto As–ICR

	Regression equation	K_2 (g/mg·h)	q_e (mg/g)	R^2
As–ICR	$\frac{t}{q_t} = 0.3483t + 0.8818$	0.1376	2.871	0.9855
NICR	$\frac{t}{q_t} = 0.512t + 0.8656$	0.3029	1.953	0.9921

where, t is the contact time (h), q_t and q_e are the amount of As(III) ions adsorbed at an arbitrary time t and at equilibrium (mg/g), respectively, and K_2 is the rate constant (h g/mg).

From the data of Figure 6, plots of t/q_t versus t for the adsorption of As(III) ions are obtained, as shown in Figure 7. The pseudosecond kinetic model rate constants for the adsorption of As(III) were summarized in Table I.

Adsorption isotherm model

Adsorption isotherms are the basic requirements for the design of an adsorbent by providing fundamental physic-chemical features.[46] The most frequently used isotherm model for adsorption experimental data correlations is the Langmuir adsorption model because of its simplicity.

To evaluate the applicability of adsorption processes as a unit operation, the initial As(III) concentrations in the range of 10-100 mg/L have been used for investigation of the adsorption isotherm (Fig. 8).

In our work, Langmuir is employed to analyze the data. The Langmuir adsorption isotherm model is based on several assumptions, including homogeneous surface, localized adsorption on the surface, and solo molecule accommodated active sites. The Langmuir isotherm equation may be written as:

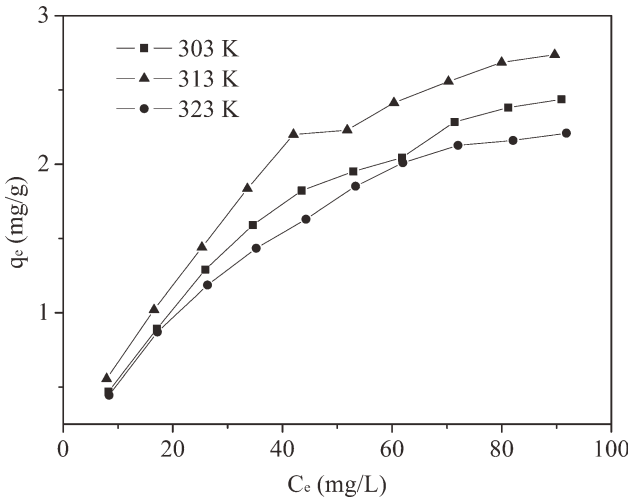

Figure 8 Effect of As(III) ions concentration on the adsorption of As(III) ions.

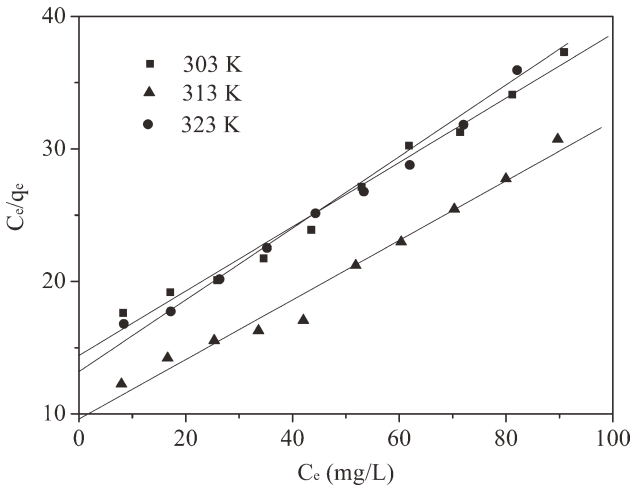

Figure 9 Langmuir adsorption isotherm model.

$$\frac{C_e}{q_e} = \frac{1}{K_b q_s} + \frac{C_e}{q_s} \tag{5}$$

where, q_e is the adsorption capacity of the resins (mg/g) at equilibrium, C_e are the concentration of As(III) in the equilibrium solution (mg/L), and q_s is the Langmuir constant, which is equal to the monolayer adsorption capacity (mg/g). The parameter K_b is the Langmuir adsorption equilibrium constant (L/mg) related to the free energy of adsorption.

The Langmuir model for the adsorption of As(III) ions onto the resins is presented in Figure 9. The straight lines of plots indicate that the adsorption processes of all cases could be well described by Langmuir adsorption model. The parameters and the correlation coefficients calculated from corresponding models were given in Table II, which indicated that the adsorption is a complex process containing physical adsorption and chemical adsorption. The adsorption process of As(III) onto As-ICR could be considered as the monolayer adsorption.

The Langmuir parameter, K_b, can be used to predict the affinity between the sorbate and sorbent using the dimensionless separation factor, R_L, defined as[47–49]:

$$R_L = \frac{1}{1 + K_b C_0} \tag{6}$$

TABLE II
Langmuir Isotherm Constants for the Adsorption of As(III) onto As–ICR

	Langmuir isotherm model			
Temperature (K)	q_s (mg/g)	K_b (L/mg)	R^2	R_L
303	4.119	0.017	0.9853	0.855
313	4.448	0.019	0.9862	0.840
323	3.697	0.018	0.9790	0.847

TABLE III
Selective Adsorption Properties of As–ICR and NICR

Elements	Distribution ratio (L/g)		Selectivity coefficient $\beta_{As^{3+}/M^{n+}}$		Relative selectivity coefficient β_r
	As–ICR	NICR	As–ICR	NICR	
As^{3+}	0.060	0.016			
Ca^{2+}	0.032	0.112	1.875	0.143	13.11
Mg^{2+}	0.015	0.071	4.000	0.225	17.78
Zn^{2+}	0.088	0.234	0.682	0.068	10.03
Cd^{2+}	0.045	0.089	1.333	0.180	7.41

$W = 0.1$ g; $V = 0.025$ L; $C0 = 50$ mg/L; $T = 40°C$; pH = 6.0.

where, R_L indicates the favorability and the capacity of the adsorbent/adsorbate system, C_0 is the initial As(III) concentration (mg/L) and K_b is the Langmuir adsorption equilibrium constant (L/mg). The R_L value classified as $R_L > 1$, $0 < R_L < 1$ and $R_L = 0$ or/and 1 suggest that adsorption is unfavorable, favorable and irreversible, respectively.[50] The values of R_L for sorption of As(III) onto As-ICR at 303, 313, 323K are greater than 0 and less than 1, indicating the favorable adsorption of As(III) onto As-ICR.

Evaluation of the selective adsorption

The selective adsorption studies were carried out under the optimal adsorption conditions to evaluate the selectivity of the resins. The distribution ratios and selectivity coefficients with respect to other metal ions using As-ICR and NICR are shown in Table III. It can be seen that the distribution ratio of As-ICR for As(III) was 3.75 times greater than that of NICR.

Furthermore, the relative selectivity coefficient of As-ICR for each individual metal ion was far greater than 1 except Zn^{2+}. These observations are attributed to the specific recognition cavities for As(III) ions created in As-ICR, which are developed by ion-imprinting effect. Based on the results shown in Table III, it is evident that As-ICR has a strong ability to selectively adsorb As(III) ions from mixed metal ions aqueous solution.

Desorption and regeneration studies

The regeneration of the adsorbent is likely to be a key factor in improving wastewater process economics. It was revealed that the adsorption capacity of As-ICR for As(III) decreased slightly from 2.16 to 1.73 mg/g with increasing the times of reuse because some adsorption sites suitable for As(III) was destroyed by HCl during the desorption process. In other words, As-ICR could be reused for five times with less than 20% regeneration loss, which indicated that As-ICR had a good reusability.

CONCLUSIONS

In summary, the adsorption of As(III) ions from aqueous solution was successfully accomplished using As-ICR. The amino groups (—NH_2) and the hydroxyl groups (C_6—OH) on CTS chains serve as the coordination sites. The maximum adsorption capacity of As-ICR for As(III) was 2.16 mg/g at pH 6.0, 40°C. Adsorption of As(III) ions onto As-ICR followed both the pseudosecond kinetic model and Langmuir adsorption isotherm model. An overall selectivity for As(III) ions was observed showing that As-ICR can be used effectively to remove and recover As(III) ions from aqueous solutions. It was also revealed that As-ICR could be reused for five times with less than 20% regeneration loss. It is the author's hope that this result will be helpful for researchers who are interested in synthesizing and applying CTS resin to remove As(III) from aqueous solution and liquid drinking as well as its derivatives in the future.

We thank to the anonymous reviewers for their comments, which significantly improved the quality of the manuscript.

References

1. Mohan, D.; Pittman, C. U. J Hazard Mater 2007, 142, 1.
2. Jain, C. K.; Ali, I. Water Res 2000, 34, 4304.
3. Rahman, M. A.; Hasegawa, H.; Rahman, M. M.; Miah, M. A. M.; Tasmind, A. Ecotoxicol Environ Saf 2008, 69, 317.
4. Hassan, K. M.; Fukuhara, T.; Hai, F. I.; Bari, Q. H.; Shafiul Islam, Kh Md Desalination 2009, 249, 224.
5. Chen, C. Y.; Chang, T. H.; Kuo, J. T.;; Chen, Y F; Chung, Y C Bioresour Technol 2008, 99, 7487.
6. Kartal, S. N.; Imamura Y. Bioresour Technol 2005, 96, 389.
7. Smith, L. K., Bruckard, W. J Int J Miner Process 2007, 84, 15.
8. Yekeler, M.; Yekeler, H. J Colloid Interface Sci 2005, 284, 694.
9. William, T.; Yasushi, T.; Atsushi S. Hydrometallurgy 2010, 105, 42.
10. Baskan, M. B.; Pala, A. Desalination 2010, 254, 42.
11. Balarama Krishna, M. V.; Chandrasekaran, K.; Karunasagar, D.; Arunachalam, J J Hazard Mater 2001, 84, 229.
12. Kim, J; Benjamin, M. M. Water Res 2004, 2053, 38.
13. Guan, B. H.; Ni, W. M.; Wu, Z. B.; Lai, Y. Sep Purif Technol 2009, 65, 269.
14. Crini, G. Prog Polym Sci 2005, 30, 38.
15. Guibal, E. Prog Polym Sci 2005, 30, 71.
16. Crini, G. Bioresour Technol 2006, 97, 1061.
17. Krishnapriya, K. R.; Kandaswamy, M. Carbohydr Res 2009, 344, 1632.
18. Juang, R. S.; Shao H. J Water Res 2002, 36, 2999.
19. Ramesh, A.; Hasegawa, H.; Sugimoto, W.; Maki, T.; Ueda, K. Bioresour Technol 2008, 99, 3801.
20. Zhou, L. M.; Wang, Y. P.; Liu, Z. R.; Huang, Q. W. J Hazard Mater 2009, 161, 995.
21. Fu, H. T.; Kobayashi, T. J Mater Sci 2010, 45, 6694.
22. Guo, T. Y.; Xia, Y. Q.; Wang, J.; Song, M. D.; Zhang, B. H. Biomaterials 2005, 26, 5737.
23. Ren, Y. M.; Wei, X. Z.; Zhang, M. L. J Hazard Mater 2008, 158, 14.

24. Liu, Y. H.; Cao, X. H.; Hua, R.; Wang, Y. Q.; Liu, Y. T.; Pang, C.; Wang, Y. Hydrometallurgy 2010, 104, 150.
25. Biju, V. M.; Mary, G. J.; Prasada, R. T. Anal Chim Acta 2003, 478, 43.
26. Garcia, R.; Pinel, C.; Madic, C.; Lemaire, M. Tetrahedron Lett 1998, 39, 8651.
27. Metilda, P.; Prasad, K.; Kala, R.; Gladis, J. M.; Prasada, R T; Naidu, G. R. K. Anal Chim Acta 2007, 582, 147.
28. Daniel, S.; Mary, G. J.; Prasada, R. T. Anal Chim Acta 2003, 488, 173.
29. Say, R.; Birlik, E.; Ersöz, A.; Yılmaz, F.; Gedikbey, T.; Denizli, A. Anal Chim Acta 2003, 480, 251.
30. Chen, H.; Olmstead, M. M.; Albright, R. L.; Devenyi, J.; Fish, R. H. Angew Chem Int Ed 1997, 36, 642.
31. Yoshida, M.; Uezu, K.; Goto, M.; Furusaki, S. Macromolecules 1999, 32, 1237.
32. Wulff, G. Angew Chem Int Ed 1995, 34, 1812.
33. Ersöz, A.; Say, R.; Denizli, A. Anal Chim Acta 2004, 502, 91.
34. Rosatzin, T.; Andersson, L. I.; Simon, W.; Mosbach, K. J. Chem Soc, Perkin Trans 2 1991, 28, 1261.
35. Dhal, P. K.; Arnold, F. H. J Am Chem Soc 1991, 113, 7417.
36. Wang, D. F.; Liu, B. J.; Xu, Y.; Zhang, L.; Li, H. Y.; Yao, H. K. 2010. Chinese patent: 201010119859.6.
37. Singh, D. K.; Mishra, S. Anal Chim Acta 2009, 644, 42.
38. Kittur, F. S.; Harish Prashanth, K. V.; Udaya Sankar, K.; Tharanathan, R. N. Carbohydr Polym 2002, 49, 185.
39. Rinaudo, M. Prog Polym Sci 2006, 31, 603.
40. Salih, B. J Appl Polym Sci 2002, 83, 1406.
41. Sun, S. L.; Wang, A. Q. Sep Purif Technol 2006, 49, 197.
42. Alakhras, F. A.; Abu, D. K.; Mubarak, M. S. J Appl Polym Sci 2005, 97, 691.
43. Reed, B. E.; Vaughan, R.; Jiang, L. J Environ Eng 2000, 126, 869.
44. Lesmana, S. O.; Febriana, N.; Soetaredjo, F. E.; Sunarso, J.; Ismadji, S Biochem Eng J 2009, 44, 19.
45. Donat, R. J Chem Thermodyn 2009, 41, 829.
46. Wang, J. L.; Chen, C. Biotechnol Adv 2009, 27, 195.
47. Hall, K. R.; Eagleton, L. C.; Acrivos, A.; Vermeulen, T. Ind Eng Chem Fundam 1966, 5, 212.
48. Huang, J. H.; Liu, Y. F.; Jin, Q. Z.; Wang, X. G.; Yang, J. J Hazard Mater 2007, 143, 541.
49. Shen, W.; Chen, S. Y.; Shi, S. K.; Xiang, X. L.; Hu, W. L.; Wang, H. P. Carbohydr Polym 2009, 75, 110.
50. Zhai, Y. B.; Wei, X. X.; Zeng, G. M.; Zhang, D. J.; Chu, K. F. Sep Purif Technol 2004, 38, 191.